Phonons in wurtzite aluminum nitride

M. Schwoerer-Böhning[a)]
Carnegie Institution of Washington, c/o Advanced Photon Source, 9700 S. Cass Ave., Argonne, IL 60439 USA
A.T. Macrander
Advanced Photon Source, Experimental Facilities Division, 9700 S. Cass Avenue, Argonne, IL 60439 USA
M. Pabst and P. Pavone
Institut für Theoretische Physik, Universität Regensburg, D-93040 Regensburg,Germany

We present data obtained with inelastic x-ray scattering measurements of the phonon dispersions in hexagonal aluminum nitride (AlN) along all three high-symmetry directions. These are the first such data for AlN. Presently available single crystals are large enough to perform an inelastic x-ray scattering experiment. The results are compared with first-principles calculations. We find excellent agreement between the data and the calculations.

The group-III nitride-based semiconductors offer great potential for applications to high-temperature electronic devices, including light emitters, diode laser structures, and detectors operating in the visible and near ultraviolet spectrum. The phonon spectrum is one of the most fundamental characteristic of these crystals. It determines their thermal and optical properties including phonon-assisted optical transitions. Therefore, a study of lattice dynamics of nitrides is not only of fundamental interest but results in a better understanding of structural parameters responsible for the efficiency of optical devices. It is suggested that the electronic and thermal properties of zinc-blende (cubic) nitrides will be superior than those of the wurtzite materials due to reduced phonon scattering in the high-symmetry crystals. The cubic nitrides are also believed to be better suited for doping than the wurtzites. However, in the bulk, group-III nitrides grow as crystals of wurtzite structure. Nitrides of the metastable cubic structure are grown as films using various techniques [1].

Theoretical work has focused on the lattice dynamics of both the cubic [2–6], and the wurtzite structure [7–10]. To our knowledge, experimental work related to phonon dispersions in wurtzite AlN has been limited to studies of the phonon density of states. Thin films have been studied by second order Raman scattering [5, 10], and powdered samples were probed using time-of-flight neutron spectroscopy [9]. The high melting temperature and the decomposition of the material at temperatures approaching the melting point make it difficult to grow large single crystals. However, wurtzite AlN is available as single crystals of reasonable size (approximately 1 mm^3) [11, 12] to perform inelastic x-ray scattering studies. Our results on the phonon dispersions in AlN are a first approach to understand the lattice dynamics in GaN and InN which require modified theoretical models accounting for the presence of 3d and 4d electrons, respectively [4].

The authors recently developed a new instrument for high-resolution inelastic x-ray scattering (HRIXS) at the Advanced Photon Source (APS) located at sector 3 of the Synchrotron Radiation Instrumentation Collaborative Access Team (SRI-CAT) [13]. The insertion device of the undulator beamline provides a typical photon flux of 3 x 109 counts/s within a band pass of approximately 5 meV at a photon energy of 13.8 keV. A spectrometer in backscattering scheme is used employing silicon (777) reflections. The data were taken with a total energy resolution of approximately 9 meV (72 cm^{-1}).

The AlN single crystal was of hexagonal shape, and had a size of approximately 0.5 x 0.5 x 0.5 mm^3. The typical width of Bragg reflections was a few hundredths of a degree. The phonon dispersions were measured in transmission (Laue geometry). Typical raw data are presented in Figure 1. The dispersions of longitudinal and transverse polarized phonons were measured along <001>, <100>, and <110> [(-A, (-M, (-K-M] directions in the (006), (300), and (220) zone. It took four days to collect the data. Not all phonon branches were measured either due to a vanishing phonon structure factor or due to limited instrumental resolution.

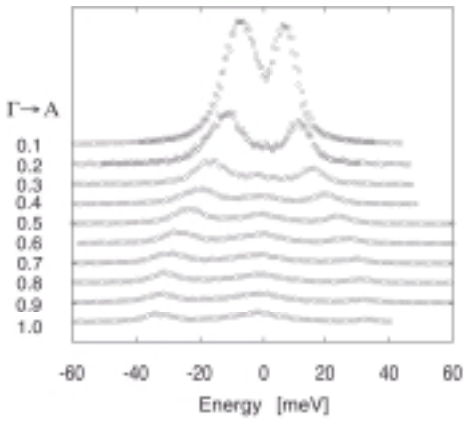

Figure 1: Transverse phonon spectra along (-A in hcp-AlN.

The calculations where performed using the plane-wave pseudopotential approach to density-functional theory (DFT) within the local-density approximation [14]. The linear-response coefficients, which allow for the

determination of dynamical matrices and, in turn, of the harmonic frequencies, are calculated within density-functional perturbation theory [15]. Interatomic force constants are obtained via Fourier deconvolution of a set of dynamical matrices calculated on an homogeneous grid in k space. Back transformation of the force constants gives phonon frequencies at arbitrary points in reciprocal space. In our calculations, we used norm-conserving pseudopotentials and basis sets including plane waves up to a kinetic-energy cutoff of 55 and 50 Ry for the calculation of static and dynamical properties, respectively. Brillouin-zone (BZ) integrations have been performed using 28 special points in the irreducible wedge of the Brillouin zone. These parameters ensure convergency of the calculated frequencies within some percent. Further calculational details are described to a larger extent in [15]. The equilibrium lattice parameters obtained by minimization of the crystal total energy of wurtzite AlN are a = 5.83 (5.88) a.u. and (c/a) = 1.599 (1.601); brackets denote the corresponding experimental values. The calculated phonon frequencies at equilibrium are shown together with our experimental data in Figure 2.

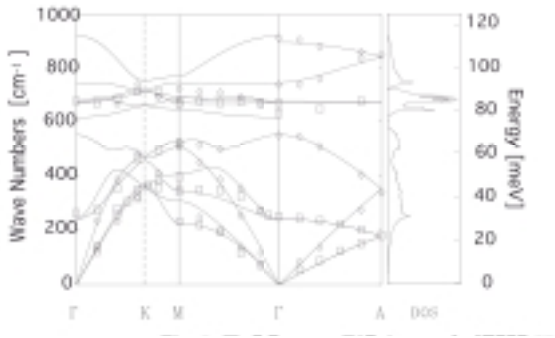

Figure 2: Longitudinal (diamonds) and transverse (squares) polarized phonon branches in hcp-AlN together with the results from *ab initio* calculations**.**

The agreement of the calculated dispersion curves with the measured points is remarkable. Minor discrepancies appear in cases where close-lying branches could not be resolved due to the instrumental resolution. With respect to other III–V semiconductors in the nitrides, one has to consider mixture of long-range Coulomb and short-range valence forces. In their work, Nipko and Loong use a rigid-ion model to calculate the phonon dispersion curves, from which they derive the phonon density of states. The first-principles calculations in this work and the calculations of Davydov *et al*. [10] (which follow a phenomenological approach) account for both the ionic and covalent forces. Only minor differences occur in the calculated phonon density of states using either approach. However, looking at the phonon disperion curves, differences become evident. Acoustic branches in the work by Nipko and Loong are less stiff than observed in our measurements. Moreover, they result in only one anticrossing (repelling) of acoustic phonon dispersion curves occurring along (- M. We conclude that current models which account for the presence of the ionic and covalent forces in nitrides result in phonon dispersion curves in agreement with our data.

Acknowledgments

We thank SRI-CAT staff of sector 3 for the performance of the beamline. We are also indebted to the management of the Experimental Facilities Division at APS. The AlN crystal was borrowed from C.M. Balkas. Use of the APS was supported by the U.S. Department of Energy, Basic Energy Sciences, Office of Energy Research, under Contract No. W-31-109-ENG-38.

Reprinted, M. Schwoerer-Böhning, A.T. Macrander, M. Pabst, and P. Pavone, *Physica Status Solidi* (b) Vol. 215, 1999, pp. 177–180.

[a)]Now at Carnegie Institue, High Pressure CAT, Argonne, 434-E.

References

[1] C. H. Hong, D. Pavlidis, S. W. Brown, and S.C. Rand, *J. Appl. Phys*. **77**, 1705 (1995).
[2] K. Karch, F. Bechstedt, P. Pavone, and D. Strauch, *Physica B* **219** and **220**, 445 (1996).
[3] J. Zi, X. Wan, G. Wei, K. Zhang, and X. Xie, *J. Phys. C* **8**, 6323 (1996).
[4] K. Karch, F. Bechstedt, and T. Pletl, *Phys. Rev. B* **56**, 3560 (1997).
[5] D.N. Talwar, *Microelectronic Engineering* **43–44**, 309 (1998).
[6] V. Yu. Davydov, Yu. E. Kitaev, I.N. Goncharuk, A.M. Tsaregorodtsev, A.N. Smirnov, A.O. Lebedev, V.M. Botnaryk, Yu. V. Zhilyaev, M.B. Smirnov, A.P. Mirgorodsky, and O.K. Semchinova, *J. Crystal Growth* **189/190**, 656 (1998).
[7] H. Siegle, G. Kaczmarczyk, L. Filippidis, A.P. Litvinchuk, A. Hoffmann, and C. Thomsen, *Phys. Rev. B* **55**, 7000 (1997).
[8] K. Karch, and F. Bechstedt, *Phys. Rev. B* **56**, 7404 (1997).
[9] J. C. Nipko and C. K. Loong, Phys. Rev. B 57, 10550 (1998).
[10] V. Yu. Davydov, Yu. E. Kitaev, I.N. Goncharuk, A.N. Smirnov, J. Graul, O. Semchinova, D. Uffmann, M.B. Smirnov, A.P. Mirgorodsky, and R.A. Evarestov, *Phys. Rev. B* **58**, 12899 (1998).
[11] C.M. Balkas, Z. Sitar, T. Zheleva, L. Bergman, R. Nemanich, and R.F. Davis, *J. Crystal Growth* **179**, 363 (1997).
[12] M. Tanaka, S. Nakahata, K. Sogabe, H. Nakata, and M. Tobioka, *Jpn. J. Appl. Phys*. **36**, L1062 (1997).

[13] M. Schwoerer-Böhning, A.T. Macrander, P.M. Abbamonte, and D.A. Arms, *Rev. Sci. Instrum*. **69**, 3109 (1998).
[14] For a review on applications of DFT to the structural properties of solids, see, e.g., W. E. Pickett, *Comp. Phys. Rep*. **9**, 115 (1989).
[15] P. Giannozzi, S. de Gironcoli, P. Pavone, and S. Baroni, *Phys. Rev. B* **43**, 7231 (1991).